

# Supplementary Document for RSS 2023 Paper

## Path Planning for Multiple Tethered Robots Using Topological Braids

### 1 Supplementary proof for Lemma 3.5

Given a polygonal trajectory  $\xi_i$  with the maximum angle of rotation  $\gamma_i$ , there exists a range of projection angles  $\alpha \in \mathcal{D} = (-\beta, -\beta + \gamma_i) \cup (\pi - \beta, \pi - \beta + \gamma_i)$ , such that the projection of  $\xi_i$  onto  $\mathcal{P}(\alpha)$ , denoted as  $\xi_i^\alpha$ , is non-monotonic with respect to  $t$ . (The authors would like to point out an error in the submitted paper: the definition of  $\mathcal{D}$  in the third line of the proof of Lemma 3.5 misses one negative sign. The definition of  $\mathcal{D}$  in this supplementary document is correct.)

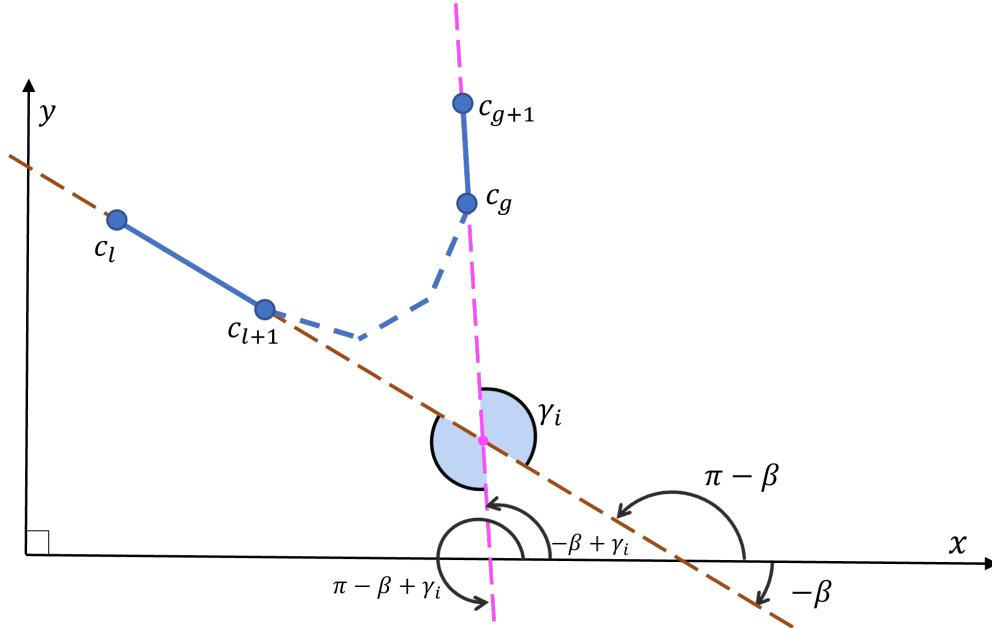


Figure 1:  $\xi_i$  projected onto the X-Y plane.

To justify the above statement, consider a polygonal trajectory  $\xi_i$  with the maximum angle of rotation  $\gamma_i$ . The projection of  $\xi_i$  onto the X-Y plane is shown in Figure 1 above, where the maximum angle of rotation occurs between the projected segments  $\overline{c_l c_{l+1}}$  and  $\overline{c_g c_{g+1}}$  (the solid blue segments), and the dashed blue lines indicate arbitrary projected segments between  $c_{l+1}$  and  $c_g$ .  $\beta$  is the acute angle between the  $x$ -axis and the extension line of  $\overline{c_l c_{l+1}}$  (the brown line). Consider a line  $\mathcal{L}(\alpha)$  obtained by rotating the  $x$ -axis by an angle  $\alpha$ . In Figure 1, the brown line is parallel to  $\mathcal{L}(-\beta)$  and  $\mathcal{L}(\pi - \beta)$ , while the pink line is parallel to  $\mathcal{L}(-\beta + \gamma_i)$  and  $\mathcal{L}(\pi - \beta + \gamma_i)$ . For each  $\alpha \in \mathcal{D} = [-\beta, -\beta + \gamma_i] \cup [\pi - \beta, \pi - \beta + \gamma_i]$ , there always exists a line parallel to  $\mathcal{L}(\alpha)$  that cuts the segments  $\overline{c_l c_{l+1}} \dots \overline{c_g c_{g+1}}$  more than once, regardless of the shape of the segments between  $c_{l+1}$  and  $c_g$ . To see this, consider a line  $\tilde{\mathcal{L}}$  passing through the intersection between the brown line and the pink line (the pink point), and passing through the interiors of two light blue-shaded arcs. In this way,  $\tilde{\mathcal{L}}$  is parallel to  $\mathcal{L}(\alpha)$  for an  $\alpha \in \mathcal{D}$ . If we shift  $\tilde{\mathcal{L}}$  vertically upwards (i.e., increasing the  $y$ -coordinate of  $\tilde{\mathcal{L}}$  at every  $x$ ) while keeping its gradient, we can move  $\tilde{\mathcal{L}}$  until it intersects with  $\overline{c_l c_{l+1}} \dots \overline{c_g c_{g+1}}$  more than once.

In 3-D, this means that there always exists a plane perpendicular to both the X-Y plane and  $\mathcal{P}(\alpha)$ , that intersects  $\xi_i$  more than once. Furthermore, since  $\xi_i$  is ascending in  $t$ , the intersections occur at different  $t$ . As a result, when  $\xi_i$  is projected onto the plane  $\mathcal{P}(\alpha)$ , there always exists a vertical line that intersects the projected trajectory  $\xi_i^\alpha$  more than once. Hence,  $\xi_i^\alpha$  is non-monotonic for  $\alpha \in \mathcal{D}$ .

## 2 Supplementary proof for Lemma 3.6

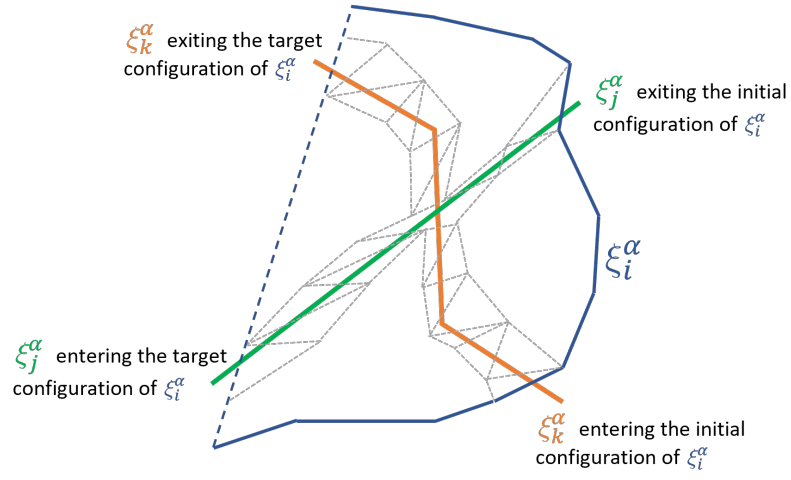
Given a non-straight polygonal trajectory, the polygon bounded by the trajectory can be partitioned into multiple triangles. There always exist a set of triangles and a sequence of evaluating the triangles for the application of elementary moves, that satisfy the following conditions:

- (1) the triangles can be classified into the four types defined in Figure 7 in the paper;
- (2) the evaluation of triangles follows a temporal sequence;
- (3) both the edges before and after an elementary move should be ascending.

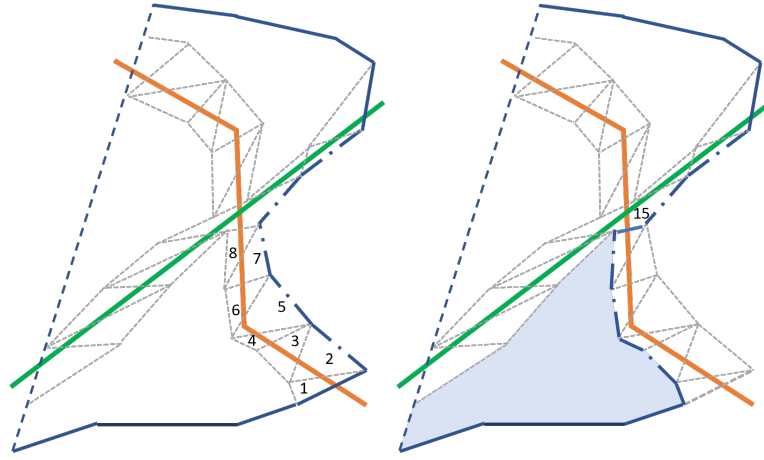
To justify the above statement, consider a non-straight polygonal projected trajectory  $\xi_i^\alpha$ , which bounds a polygon region that contains the projections of other trajectories. Figure 2(a) in this document shows an example, where two projected trajectories  $\xi_j^\alpha$  and  $\xi_k^\alpha$  pass the interior of the polygon bounded by  $\xi_i^\alpha$  (the blue line segments). Suppose we would like

to obtain a sequence of elementary moves that transform  $\xi_i^\alpha$  into a straight line (the dashed line segment). We can construct two chains of triangles that fully contain  $\xi_j^\alpha$  and  $\xi_k^\alpha$ , as shown in Figure 2(a). A type I triangle is at the intersection between trajectories  $j$  and  $k$ , while all other triangles are of type II or III. The intersections between  $\xi_i^\alpha$  and the other two trajectories separate  $\xi_i^\alpha$  into three parts; we pick the part bounded by two intersection points and transform it, using a sequence of elementary moves, to the boundary of the chain containing the lower section of  $\xi_k^\alpha$  and the upper section of  $\xi_j^\alpha$  (the dash-dotted blue line in Figure 2(b)). This transformation can be done because the area bounded by the initial and the transformed trajectories is empty and can be partitioned into triangles of type IV. Furthermore, both the initial and the transformed trajectories are ascending. Then, the chain of triangles containing trajectory  $k$  can be evaluated following a permissible sequence indicated by the numbering in Figure 2(b). If elementary moves can be applied to all these triangles, trajectory  $i$  can be further transformed to the configuration shown in Figure 2(c). Notice that in triangle 15, trajectory  $j$  crosses trajectory  $k$ . Hence, in order to evaluate triangle 15, the temporal sequence requires the lower section of trajectory  $j$  to be evaluated first. To do so, the lower part of trajectory  $i$  is further transformed to the boundary of the chain containing the trajectory  $j$  (Figure 2(d)). This is possible because the blue region in Figure 2(c) is empty. Then, the sequence of triangles 10 to 18 can be evaluated and results in a transformed trajectory in Figure 2(e) if elementary moves are successfully applied to all triangles. To finish the transformation, the following steps can be followed. First, transform the upper section of trajectory  $i$  to the boundary of trajectory  $j$  by applying elementary moves to the orange region in Figure 2(e). Second, apply a sequence of evaluations to the chain of triangles 19 to 25. Finally, transform trajectory  $i$  across the empty space illustrated by the green region. Note that the temporal sequence of evaluation is respected throughout the transformation process; furthermore, the transformed trajectory in every step is ascending.

From the above example, we can obtain a general treatment for a non-straight projected trajectory  $i$ . First, construct a chain of triangles for each of the trajectories in the interior of the polygon bounded by trajectory  $i$ ; the triangles are of type I, II, or III. Pick a section of the trajectory  $i$  and transform it across the empty space, until the transformed trajectory becomes the boundary of a chain. Evaluate the triangles in the chain from the bottom to the top, until a triangle is encountered that contains a crossing between two trajectories. For the lower part of trajectory  $i$  that has been transformed across the chain, continue to transform it across the empty space, until reaching the boundary of another chain. Evaluate the triangles in the chain from the bottom to the top, until meeting a triangle that contains

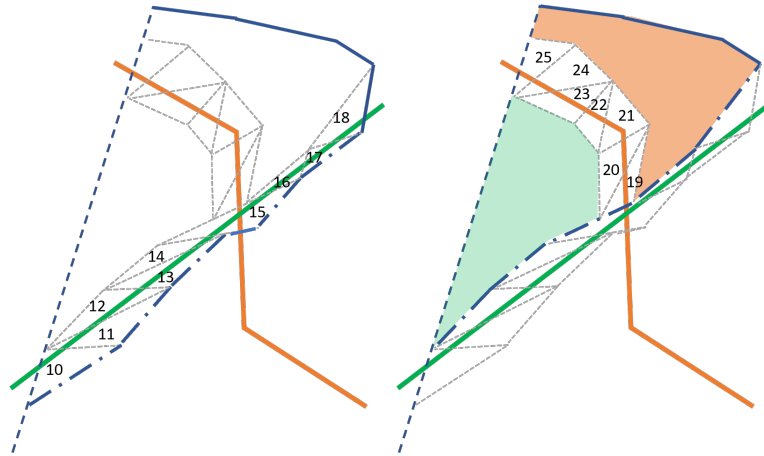


(a)



(b)

(c)



(d)

(e)

Figure 2: A sequence of transformations of trajectory  $i$ .

a crossing point. Check whether the lower sections of the two crossing trajectories have been evaluated; if yes, the triangle containing the crossing point can be evaluated; if not, continue to transform the lower part of the trajectory  $i$  until meeting the boundary of another chain, and evaluate the chain of triangles. This procedure can be conducted iteratively until trajectory  $i$  is successfully transformed into a straight line, or a triangle is encountered to which the elementary move cannot be applied (a tangle).

### 3 Table 1: Precomputed list of possible 3-braids with length 3 and 4

Length 3	subsequent braids with length 4	actions
$\sigma_1\sigma_2\sigma_1$	$\sigma_1\sigma_2\sigma_1\sigma_2$	rejected because equivalent to $\sigma_2\sigma_1\sigma_2\sigma_2$
	$\sigma_1\sigma_2\sigma_1\sigma_2^{-1}$	reduced to $\sigma_2\sigma_1$
$\sigma_1\sigma_2\sigma_1^{-1}$	$\sigma_1\sigma_2\sigma_1^{-1}\sigma_2$	rejected because equivalent to $\sigma_2^{-1}\sigma_1\sigma_2\sigma_2$
	$\sigma_1\sigma_2\sigma_1^{-1}\sigma_2^{-1}$	reduced to $\sigma_2^{-1}\sigma_1$
$\sigma_1\sigma_2^{-1}\sigma_1$		equivalent to a 3-braid tangle, rejected
$\sigma_1\sigma_2^{-1}\sigma_1^{-1}$	$\sigma_1\sigma_2^{-1}\sigma_1^{-1}\sigma_2$	rejected because equivalent to $\sigma_2^{-1}\sigma_1^{-1}\sigma_2\sigma_2$
	$\sigma_1\sigma_2^{-1}\sigma_1^{-1}\sigma_2^{-1}$	reduced to $\sigma_2^{-1}\sigma_1^{-1}$
$\sigma_1^{-1}\sigma_2^{-1}\sigma_1$	$\sigma_1^{-1}\sigma_2^{-1}\sigma_1\sigma_2$	reduced to $\sigma_2\sigma_1^{-1}$
	$\sigma_1^{-1}\sigma_2^{-1}\sigma_1\sigma_2^{-1}$	rejected because equivalent to $\sigma_2\sigma_1^{-1}\sigma_2^{-1}\sigma_2^{-1}$
$\sigma_1^{-1}\sigma_2^{-1}\sigma_1^{-1}$	$\sigma_1^{-1}\sigma_2^{-1}\sigma_1^{-1}\sigma_2$	reduced to $\sigma_2^{-1}\sigma_1^{-1}$
	$\sigma_1^{-1}\sigma_2^{-1}\sigma_1^{-1}\sigma_2^{-1}$	rejected because equivalent to $\sigma_2^{-1}\sigma_1^{-1}\sigma_2^{-1}\sigma_2^{-1}$
$\sigma_1^{-1}\sigma_2\sigma_1$	$\sigma_1^{-1}\sigma_2\sigma_1\sigma_2$	reduced to $\sigma_2\sigma_1$
	$\sigma_1^{-1}\sigma_2\sigma_1\sigma_2^{-1}$	rejected because equivalent to $\sigma_2\sigma_1\sigma_2^{-1}\sigma_2^{-1}$
$\sigma_1^{-1}\sigma_2\sigma_1^{-1}$		equivalent to a 3-braid tangle, rejected
$\sigma_2\sigma_1\sigma_2$	$\sigma_2\sigma_1\sigma_2\sigma_1$	rejected because equivalent to $\sigma_1\sigma_2\sigma_1\sigma_1$
	$\sigma_2\sigma_1\sigma_2\sigma_1^{-1}$	reduced to $\sigma_1\sigma_2$
$\sigma_2\sigma_1\sigma_2^{-1}$	$\sigma_2\sigma_1\sigma_2^{-1}\sigma_1$	rejected because equivalent to $\sigma_1^{-1}\sigma_2\sigma_1\sigma_1$
	$\sigma_2\sigma_1\sigma_2^{-1}\sigma_1^{-1}$	reduced to $\sigma_1^{-1}\sigma_2$
$\sigma_2\sigma_1^{-1}\sigma_2$		equivalent to a 3-braid tangle, rejected
$\sigma_2\sigma_1^{-1}\sigma_2^{-1}$	$\sigma_2\sigma_1^{-1}\sigma_2^{-1}\sigma_1$	rejected because equivalent to $\sigma_1^{-1}\sigma_2^{-1}\sigma_1\sigma_1$
	$\sigma_2\sigma_1^{-1}\sigma_2^{-1}\sigma_1^{-1}$	reduced to $\sigma_1^{-1}\sigma_2^{-1}$
$\sigma_2^{-1}\sigma_1^{-1}\sigma_2$	$\sigma_2^{-1}\sigma_1^{-1}\sigma_2\sigma_1$	reduced to $\sigma_1\sigma_2^{-1}$
	$\sigma_2^{-1}\sigma_1^{-1}\sigma_2\sigma_1^{-1}$	rejected because equivalent to $\sigma_1\sigma_2^{-1}\sigma_1^{-1}\sigma_1^{-1}$
$\sigma_2^{-1}\sigma_1^{-1}\sigma_2^{-1}$	$\sigma_2^{-1}\sigma_1^{-1}\sigma_2^{-1}\sigma_1$	reduced to $\sigma_1^{-1}\sigma_2^{-1}$
	$\sigma_2^{-1}\sigma_1^{-1}\sigma_2^{-1}\sigma_1^{-1}$	rejected because equivalent to $\sigma_1^{-1}\sigma_2^{-1}\sigma_1^{-1}\sigma_1^{-1}$
$\sigma_2^{-1}\sigma_1\sigma_2$	$\sigma_2^{-1}\sigma_1\sigma_2\sigma_1$	reduced to $\sigma_1\sigma_2$
	$\sigma_2^{-1}\sigma_1\sigma_2\sigma_1^{-1}$	rejected because equivalent to $\sigma_1\sigma_2\sigma_1^{-1}\sigma_1^{-1}$
$\sigma_2^{-1}\sigma_1\sigma_2^{-1}$		equivalent to a 3-braid tangle, rejected